

# **Violin bow and string dynamics measured with a mechanical bowing machine**

John S. Lamancusa  
Mechanical Engineering Department,  
The Pennsylvania State University,  
329 Leonhard Bldg,  
University Park, PA 16802

## **Abstract**

A mechanical bowing machine is described for studying the complex dynamic interaction between a violin bow and string. Bowing parameters (force, velocity and distance from the bridge) are precisely controlled. The machine is used to study the effect of bowing parameters on the steady state motion of a string mounted on a monocord, and the tip vibration of the violin bow. Differences between three different string brands, and eight bows of different materials (Pernambuco, graphite composite and metal) and monetary value are also investigated.

## **I. INTRODUCTION**

While the dynamic responses of the violin and bowed string have been studied in detail, the bow has received far less attention. Perhaps this is due to its seemingly-simple construction, a bundle of horse hair held in tension by a wooden stick. However despite this apparent simplicity, it is not possible to deduce the quality or value of a bow from a simple physical measurement. From an acoustic standpoint, bows differ in their measurable static and dynamic properties including: weight, balance point, material density, elastic modulus, camber, graduation, stiffness, damping, and vibrational modes. These properties have been studied by several researchers [1-5] and related to subjective ratings of bow quality [6]. However it is still not known how these physical properties directly relate to playing characteristics or contribute to making a better bow. One impediment to studying these complex relations in a controlled scientific manner is the inability of a player to achieve perfectly consistent and repeatable bow strokes.

The intent of this work is to investigate how a bow generates motion in a string, using a mechanical bowing machine designed to achieve consistent, repeatable bow strokes of controlled speed, contact force and position relative to the bridge. The machine described here is portable, does not alter the dynamic properties of the bow and requires no modification to the bow or instrument. It is used to compare a diverse collection of bows of different material (Pernambuco, Brazilwood, carbon fiber, hollow steel) and wide range of monetary value (\$60 modern import, modern handmade and rare old French). The usefulness of the machine is further demonstrated by comparing different strings brands. This work is a step toward understanding how the

physical properties of a bow affect its playability and sound quality. It is hoped that such an understanding will help bow makers to produce bows of consistently superior playability.

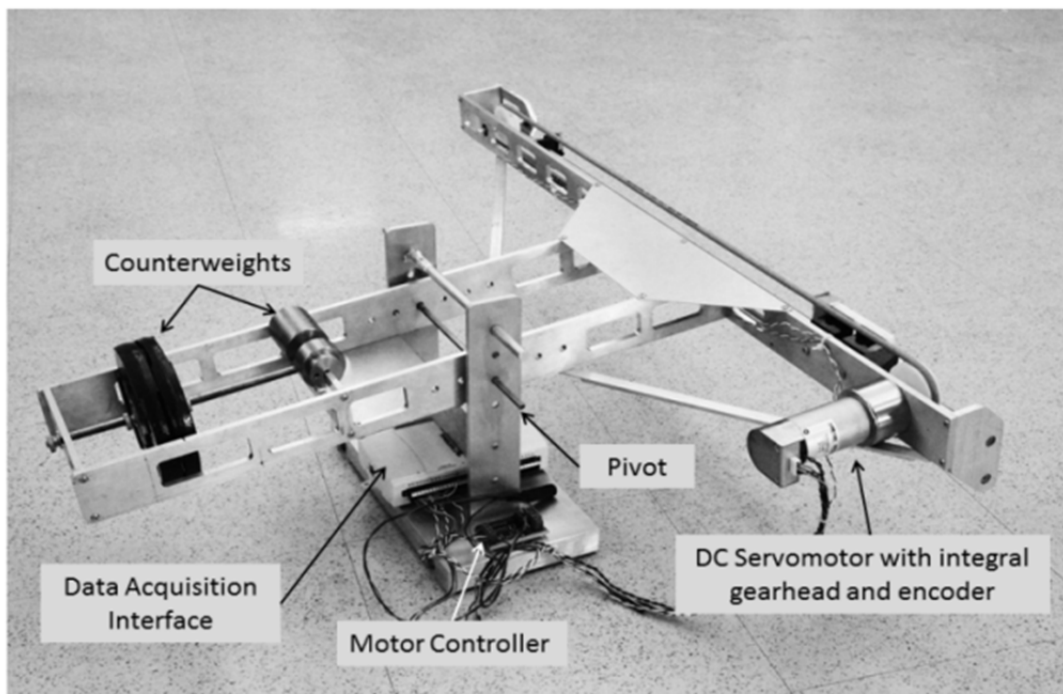
Several mechanical bowing machines have been developed by multiple researchers to study the stick-slip motion of the bowed string which was first described by Helmholtz in 1862 [7]. C. V. Raman [8] used a machine that moved a violin under a stationary bow. The contact force between bow and string, controlled by a counterweight, varied slightly over the length of the bow stroke. Saunders [9] used a rotating, rosined celluloid disc to compare response curves of violins. Schelleng [10] investigated the range of bow velocity, pressure, and distance from the bridge needed to achieve stable Helmholtz motion using a machine similar to Saunders'. Another approach to mechanical bowing has been to use a loop or belt of rosined hair mounted between two pulleys. Several researchers [11-13] have used this technique to study the acoustic radiation and mechanical response of violins. Bladier [14] used a rotating disc of hard rubber with a rosined edge. Lawergren [15] moved a bow with wagons attached at the tip and frog. Contact force was adjusted by pressing the violin upward against the bow by a screw jack. Pickering [16] also used a bow driven by a DC servomotor. Downward force was controlled by a weighted roller contacting the back of the stick at the point of bowing. Both of these machines were intended to study string motion, not bows. They would alter the dynamic properties of the bow due to the manner in which it was supported. Schumacher [17] used a stationary bow and moved the violin with a lead screw. The bowing force was measured by strain gages in the bow grip and was controlled with a torque motor. Cronhjort [18] modified a computer printer to provide linear bow motion using a stepper motor, while a mechanical actuator controlled the force. This machine has been used by several researchers to confirm Schelleng's data with a real violin bow [19], to study the startup transient at the beginning of the bow stroke [20], and to investigate the influence of bow modes and damping [21]. Woodhouse, Schumacher and Garoff [22,23] moved a rosined glass rod with a linear motion apparatus to study the friction characteristics of rosin. Contact force was controlled by two micrometer screws at each end of the string. String force at the bridge was measured by a dual piezo-ceramic sensor. Galluzzo [24,25] used a DC servomotor to control the linear motion of a rosined acrylic (PMMA) rod. Force and velocity were dynamically controlled by a closed-loop digital system. This apparatus was used to study pre-Helmholtz transients and bowing force limits of cellos. An alternative approach to directly controlling bowing parameters with a machine is to measure what a player actually does by a combination of motion capture and sensors [26-28].

## **II. TEST APPARATUS**

### **A. Bowing Machine Design and Tradeoffs**

The design of any machine is a delicate balance of tradeoffs, and satisfaction of multiple competing objectives, including complexity, accuracy and cost. To be most useful, a mechanical bowing machine must be able to move an actual bow relative to a string with repeatable

acceleration, speed, downward force, distance to the bridge, and tilt, without altering the dynamic properties of either the bow or the violin. A machine which achieves these design objectives is illustrated in Figure 1. The bow is mounted in a three point grip, emulating the points of contact with a player's hand. The bow can be rotated in the grip to alter its tilt (hair flatness) relative to the string. The grip has adjustments for level and horizontal alignment. The grip carriage is constrained to move parallel to and at a constant distance from a pivot. The pivot axis is oriented parallel to the longitudinal axis of the bow. Smooth linear motion is obtained with three linear bushings on two polished stainless guide rods. Linear ball bearings were initially tried but generated too much mechanical noise. A permanent magnet DC servomotor with integral gearhead and optical encoder (Pittman GM9236SO19-R1, 12VDC, gear ratio 19.7:1) moves the carriage by means of grooved pulleys and a nylon belt. Initially, a stepper motor was tried, but the steps caused unacceptable audible noise, vibration and jerkiness which interfered with the Helmholtz motion of the string.



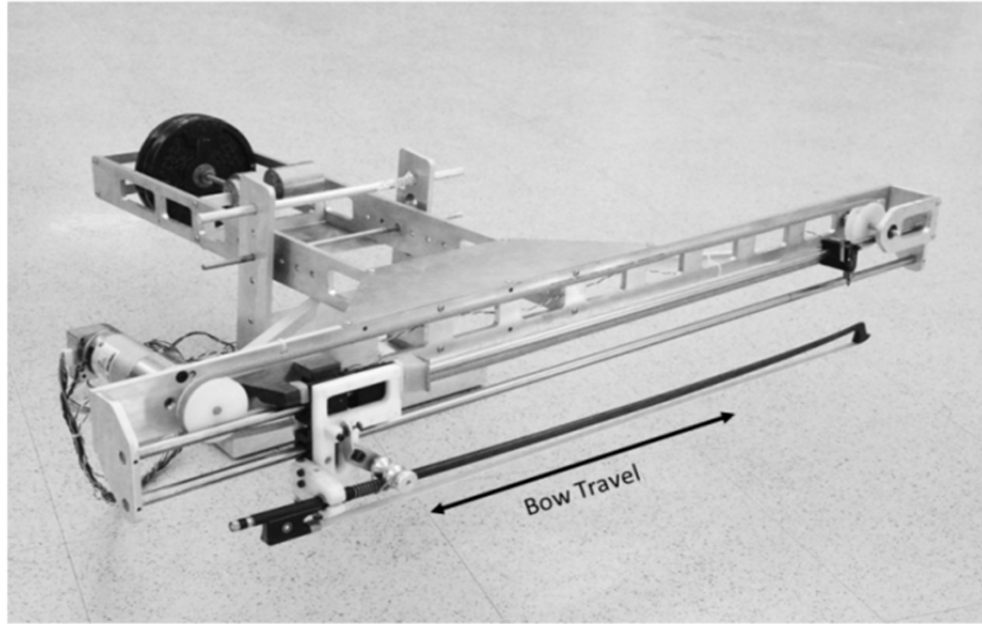


Figure 1. Mechanical bowing machine to achieve controllable force, velocity and bowing distance from bridge a) side view b) front view

While it may be possible to actively control bowing force using an electromagnetic shaker, this apparatus is designed to exert a constant downward force across the entire bow stroke using a simpler, fail-safe, passive mechanism. Inspired by the tone-arm of a record turntable, constant force is achieved by a counterweight at a fixed distance from the pivot point. Ball bearings provide support at the pivot with a minimum of friction. Weight can be easily added or subtracted, and the moment arm can be varied by a lead screw to adjust the contact force between bow and string. Since the center of gravity of the bow is always at the same distance from the pivot, Newton's Second Law dictates that the downward force between bow and string is constant regardless of the lateral position of the bow carriage. Careful attention was also given to positioning the pivot point as close as possible to the midpoint between the counterweight and the plane of the bow. This insures that the static contact force remains constant as the frame rotates about its pivot. If the moment arms were unequal, the machine would only balance at one angular position.

This passive design sacrifices the ability to dynamically control contact force for the sake of simplicity (mechanical, electrical and programming), reliability, and safety of the instruments being tested. There are many important and useful investigations that do not require the complexity and cost of dynamic force control. As noted by [galluzo thesis ], with a computer-controlled mechanical shaker powerful enough to provide the required dynamic forces, there is always the possibility of things going awry, causing damage to the instrument.

When properly adjusted, the variation of force is within  $\pm 0.1$  g across the entire bow stroke. It should be noted that if the bow carriage pivots up or down during a test, as it would if the bow tension is very low or the bow is excessively flexible, there can be a dynamic loading effect as the bow moves against the inertia of the frame. Low bow tension will cause the contact force to decrease toward the center of the stroke, and then increase at the end of the bow stroke. For bows at normal playing tension, this has not been a problem.

A digital scale (Ohaus Scout-Pro) was used to measure the downward force. When using an actual violin, the downward force can be measured by supporting the violin directly on the scale while it is being bowed. When the monocord with granite base was used, its weight exceeded the static load capacity of the scale. In this case, the downward force at the center of the bow was measured before and after each test, with the monocord removed.

The frame elements are machined of 6061 aluminum. Excess material was removed where possible to minimize weight. The weight of the sliding bow carriage was optimized to minimize inertia and maximize acceleration. An earlier prototype of the machine was constructed of hardwood. The major advantages of wood are ease of manufacture and low weight, but warping due to humidity changes caused unacceptable distortion.

The bow motion is controlled by a National Instruments data acquisition and interface (DAQ) module (NI USB-6211) connected by USB interface to a personal computer. The control program, written in Labview, allows the user to specify the desired acceleration rate and steady state velocity. An optical encoder (HP, 500 pulses/rev) mounted on the motor provides rotary position feedback to a PD (Proportional/Derivative) velocity control loop. Integral feedback would result in unstable velocity control. The feedback gains were chosen empirically to minimize overshoot and rise time. The time step of the controller is 10msec. The resulting output voltage is converted to a pulse-width-modulated (PWM) signal by a Syren 10 motor controller which provides current to the servomotor. The motion ends when the carriage reaches a mechanical stop and trips a mechanical limit switch, resetting the program for the next bow stroke. The maximum values of velocity and acceleration respectively are 60 cm/sec and  $300 \text{ cm/sec}^2$ . The total stroke is adjustable, with a maximum value of 58 cm. Velocity is measured by an optical encoder on the motor, not directly at the bowing point. The time history of velocity is stored to a file for later processing.

The digital speed control has a measured maximum overshoot of 3% or less. In the steady state, the standard deviation of velocity is less than 1%. There are slight variations from a perfect straight line in the acceleration portion, possibly due to cycle-to-cycle variations inherent in a digital control scheme. It is likely, but cannot be proven, that the inertia of the gearing, bow carriage and the flexibility of the belt would prevent these small perturbations from appreciably affecting the velocity at the bowing point.

## **B. Summary of Machine Features**

The features of this bowing machine include:

1. It uses an actual bow, not a belt or disc.
2. It can be used on a real instrument (violin, viola or cello), or a monocord.
3. The bow is held in a lifelike manner at the frog. No alteration or modifications to the bow are needed.
4. Force, tilt and bowing distance to bridge are precisely controlled by a simple, passive mechanical apparatus.
5. Bow speed and acceleration rate are user selectable and digitally controlled.
6. Data is captured digitally and stored for later signal processing.
7. The system is self-contained and portable.

The primary limitation of this machine is that it cannot achieve bouncing or non-constant force gestures, because the magnitude of the contact force is passively controlled by the position of a static counterweight.

## **C. Monocord Design**

It is well known that the violin is an extremely complicated dynamic system. Each violin has a distinct signature of mode shapes and natural frequencies which can potentially interact with the dynamics of the bow. Since the intent of this study was to investigate bows, it was decided to minimize this complexity and use a single string “monocord”. The monocord shown in Figure 2 consists of a solid aluminum bar (1.3 x 2.5 x 45.7 cm) attached by adhesive to a solid granite base (10.2 x 3.1x45.7 cm). The granite base is supported on rubber feet to minimize coupling with the supporting table. The single string is supported between aluminum bridges. A planetary gear peg (Wittner) provides fine-tuning adjustment. While it is impossible to achieve a totally inert string support, the monocord is designed to be as rigid and non-resonant as possible. The string length (L) can be adjusted by moving the bridge, and was set to 330mm. Any violin string type or gage can be used. The string is tuned with the aid of a Korg electronic tuner (model CA-40) and Wittner clip-on pickup attached to the tuner peg. The effectiveness of the monocord at isolating string motion from its base is demonstrated by the fact that the tuner clipped to the peg has difficulty measuring a sufficient signal to lock onto. The bowing distance from the bridge (B) is measured to the far edge of the hair band and is set by an adjustable guide. The monocord is also superior to a complete violin because it is easier to adapt for a string displacement sensor.

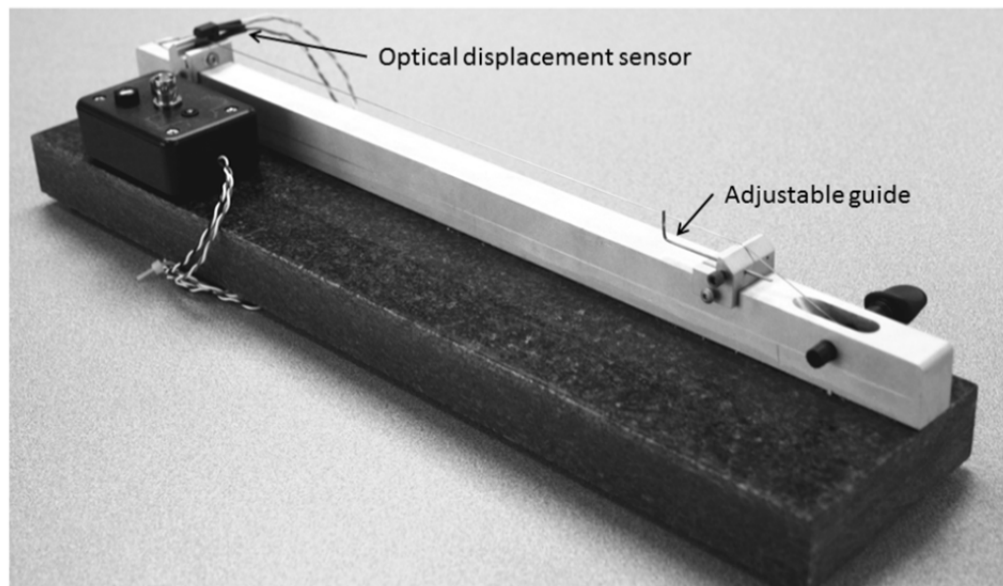


Figure 2. Monocord, with string displacement sensor at upper left, and adjustable guide to set the distance from bowing point to bridge at lower right

#### D. Instrumentation

Simultaneous measurements are made of the horizontal displacement transverse to the string, and the acceleration of the bow tip in the direction of the bow hair. The string vibration is measured by an optical sensor (Fairchild H22A1) mounted 4.5mm from the bridge (see Figure 2). The sensor provides an output of 5.0V/mm, has a useful linear range of  $\pm 0.1$ mm, and needs no amplification. Compared to other types of transducers such as magnetic pickups [19] or bridge force sensors [29, 30], optical sensors have some distinct advantages including: direct measurement of string displacement, low noise, low cost, simple electronics, no effect on string motion, very small sensing aperture (nominal sensing area is 0.9mm wide), and measurement of string motion in the horizontal direction only. However, the sensor placement relative to the bridge will affect the waveform shape and amplitude, as well as its frequency content. Moving closer to the bridge steepens the flyback portion of the measured N wave, but decreases the overall amplitude. The chosen distance was found to be an acceptable compromise. The theoretical difference in frequency content between the output of an optical sensor placed 4.5mm from the bridge, and the force at an infinitely rigid bridge (perfect N wave), is less than 1 dB for frequencies less than 5.8kHz, and 3.3dB at 10 kHz. If the intent were to infer the actual bridge force using the optical pickup measurement, it would have to be corrected for distance and bridge admittance. However, since the objective of this study is to compare string motion under different bowing conditions or with different bows, all measurements will be affected equally and there is no need for this correction and the many assumptions that would underlie those corrections.

A miniature piezoelectric accelerometer (PCB model 352A73, 0.3g mass) is mounted with wax at the bow tip to measure the acceleration in the direction of the hair. A battery-powered ICP supply (PCB 480D06) provides excellent signal to noise ratio and a voltage output of 4.22 mv/g. Test results with and without the accelerometer in place, showed no measurable effect on the string motion. Adding 0.3g (the same mass as the accelerometer) at the bow tip causes a very small change in the frequency of the first stick mode from 79.75 to 79.25 Hz, a change of -0.6%. Therefore, for the purposes of these tests, the dynamic effect of accelerometer mass is considered negligible. The static weight is easily balanced out by the counterweight. Voltage signals from the two sensors are simultaneously recorded by a Zoom H4n digital recorder. Data is encoded at 48kHz and stored in uncompressed .wav files for later analysis.

### **E. Data Analysis**

Data files are processed using a custom MATLAB program. The time histories of the string motion and the bow tip vibration are synchronized by correcting for the acoustic travel time of the transverse wave on the string from the bowed point to the string sensor. No attempt is made to correct for the continuously changing distance on the hair from the bowing point to the tip. The RMS level is calculated directly from the time history. The Fast Fourier Transform (FFT) is calculated and averaged for each channel. The number of averages is user-selectable. The number of data points per FFT ( $N=7192$ ) was chosen to make the fundamental note of the D string (293.66 Hz) coincide exactly with a discrete FFT bin. The FFT provides amplitude at discrete frequency increments ( $\Delta f$ ) of 6.674 Hz. The length of each time average is 0.1498 seconds. A flat top spectral window further minimizes leakage error. While the FFT theoretically yields valid data up to the Nyquist frequency (half the sampling frequency), for this application all data above 10KHz are not significant and therefore ignored.

Since the actual measured quantities are string displacement and bow tip acceleration, the FFT spectra are converted to velocity so that they may be compared to each other in the same units. This conversion is performed in the frequency domain by dividing by frequency  $\omega$  (radians/sec) to convert from acceleration to velocity or multiplying by  $\omega$  to convert from displacement to velocity.

The spectral centroid is used to measure the location of the “center of mass” of the signal. It is commonly used in digital audio processing as a measure of the timbre or brightness of a sound [31], and has been applied to violins [32]. The spectral centroid is calculated for the string velocity spectrum and for the bow tip velocity spectrum over the frequency range of 0 to 10 kHz. Frequency centroid is a single quantity which is easy to calculate. However, more detailed measures, such as loudness levels in critical bands, may be required to better correlate with human perception.



### **III. EXPERIMENTAL RESULTS**

#### **A. Test Procedure**

It was found through experience that special care must be taken to control all variables as much as possible to insure repeatable results. Prior to each test, rosin is cleaned from the string using a cotton cloth. One swipe of rosin is then applied to the bow hair and approximately 20 up/down strokes are made on the string to settle things in. The same rosin (Hill light) is used for all tests. A new string that had been under tension for a period of several days, is used to minimize the effect of changing string properties. All tests use a D'Addario Helicore medium gage D string unless otherwise noted. The bow hair is flat on the string. The hair is tensioned to a spacing of 7.5mm at the point of closest approach to the stick. The width of the hair ribbon is  $\approx 10$ mm. The distance to the bowing point (B) is always measured from the bridge to the edge hair ribbon farthest from the bridge. A minimum of five seconds delay is used between successive tests, to allow any vibrations in the machine to die out. Between tests, the string tuning is checked and corrected if necessary. The contact force is measured with a digital scale before and after each test. Humidity can have an effect on rosin behavior and the resulting response of a bowed string. Unfortunately, humidity could not be controlled in the room where the machine is located. It is measured for each test session, and every attempt is made to perform all related tests at the same humidity.

#### **B. Steady State Response**

Tests were performed on a hand-made modern Pernambuco bow (Rodney Mohr) to develop a basic understanding of the bow/string interaction. Typical time history and FFT data are shown in Figure 3 at the middle of a downbow stroke. The steady-state Helmholtz motion of the string is clearly seen. The tip's time response appears to be amplitude-modulated at the fundamental frequency of the D string (293.66Hz). The almost total absence of the fundamental tone in the tip's frequency response is noteworthy. Typical of bowed string motion, peaks in the FFT occur at the fundamental note and its integer harmonics. Stripping away all but the amplitudes at the FFT peaks removes extraneous clutter and results in a simplified plot. Unless otherwise noted, all subsequent FFT plots show only the amplitudes of the harmonic peaks.

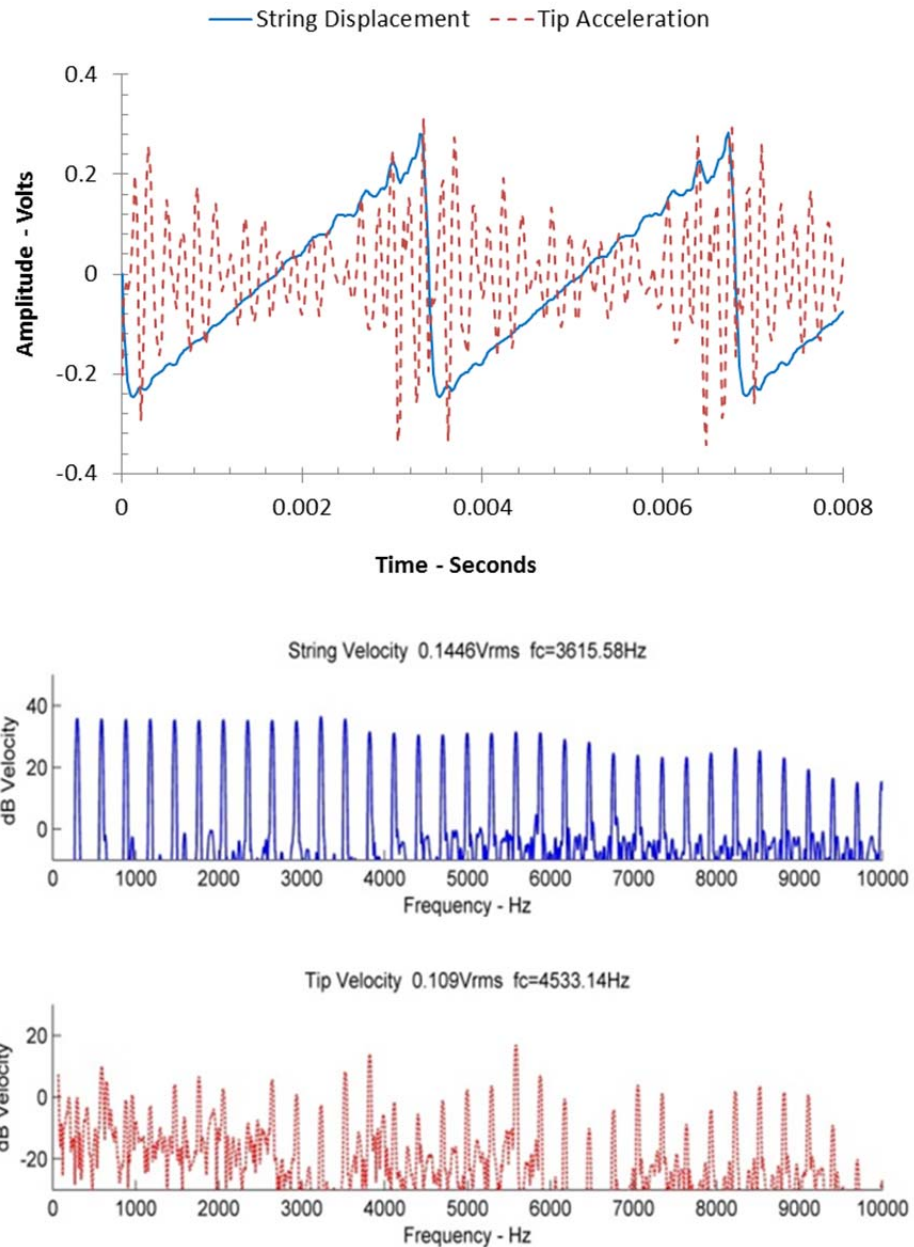


Figure 3. Steady state response at middle of bow stroke ( $W=80g$ ,  $V=20$  cm/sec,  $B=30mm$ ), string motion is measured 4.5 mm from the bridge opposite the bowing point a) Time history b) Frequency response (FFT) of string velocity c) Frequency response (FFT) of bow tip velocity

The variation with time of the frequency response for an entire bow stroke from frog to tip is graphically shown in the “waterfall” plots of Figure 4. These 3-dimensional plots display a time sequence of 2-D FFT plots (amplitude vs frequency), with the third axis being time. The string response is observed to be relatively uniform with time, while the bow tip response exhibits a much more complicated behavior over the length of the bow stroke. However, this does not

appear to affect the string motion.

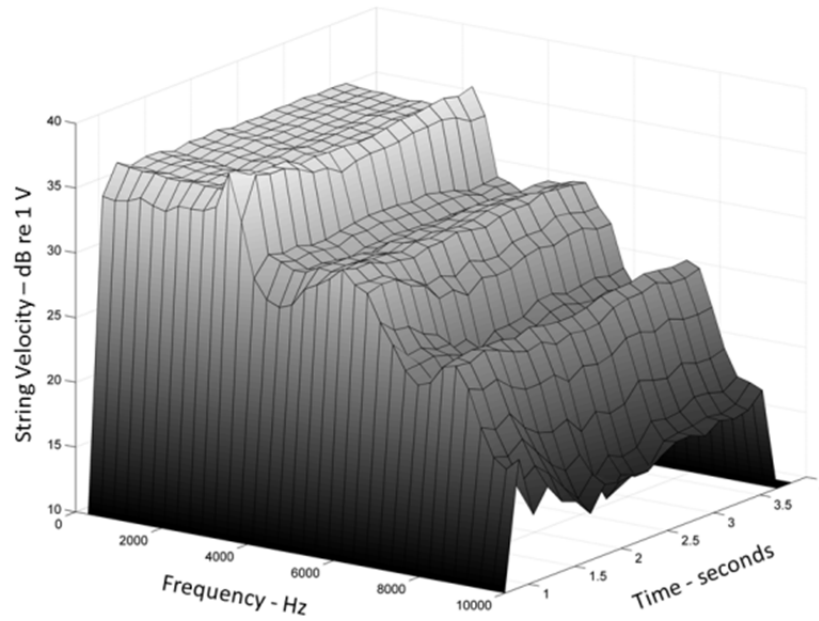


Figure 4a. Time variation of frequency spectra (waterfall plot) of string velocity over down bow stroke from frog to tip

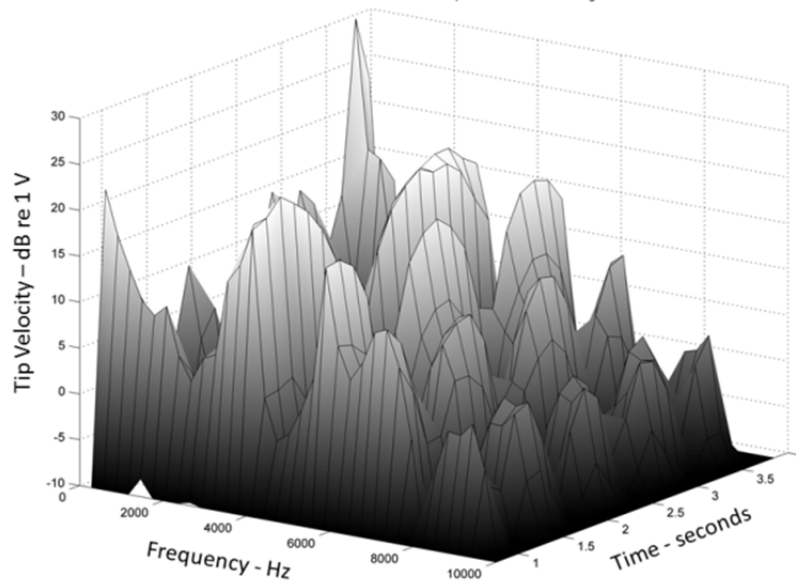


Figure 4b. Time variation of frequency spectra (waterfall plot) of bow tip velocity over down bow stroke from frog to tip

While it is well known that the sound radiated from a violin is directly related to the natural frequencies and mode shapes of the instrument body, it is less clear that the same statement can be made for the effect that the bow has on string motion. As noted by Guettler and Askenfelt [21], the characteristic impedance of the bow hair in the longitudinal direction is at least an order of magnitude higher than the string. Therefore, the string motion will not efficiently couple to the hair, except possibly at resonant frequencies of the stick. However, they could find no clear evidence that bow resonances are excited sufficiently to have a significant influence on string response.

To look for evidence of coupling between stick modes and the bowed string response, a frequency response test was performed on the bow while mounted on the bowing machine. A miniature accelerometer was placed on the tip and an instrumented hammer struck the tip in the longitudinal direction of the hair. The measured frequency response is shown in Figure 5a and compared to the string and tip responses (mechanically bowed) for a test condition of 80g, 20 cm/sec and 30mm bowing distance. There is no apparent correlation between the curves. The same frequency response is then compared to the tip vibration response (mechanically bowed) for 3 different bowing distances from the bridge in Figure 5b. While there is a large change in the tip frequency response due to bowing distance, no consistent discernible effect can be seen at the natural frequencies of the stick.

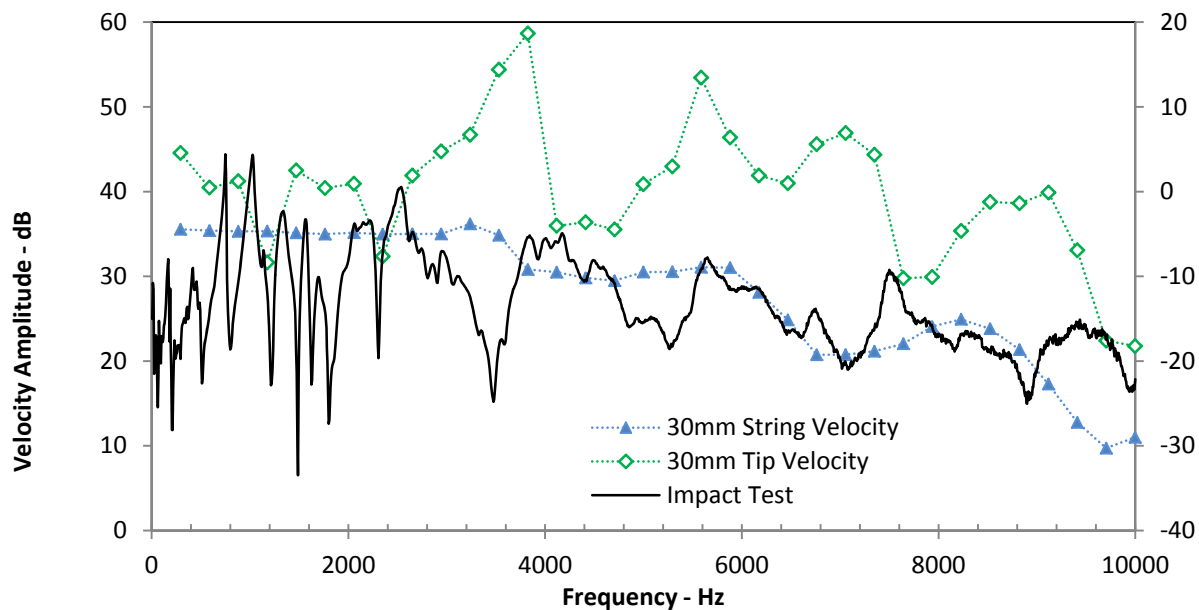


Figure 5a. Comparison of bowed string and tip frequency response to bow natural frequencies determined by impact hammer test

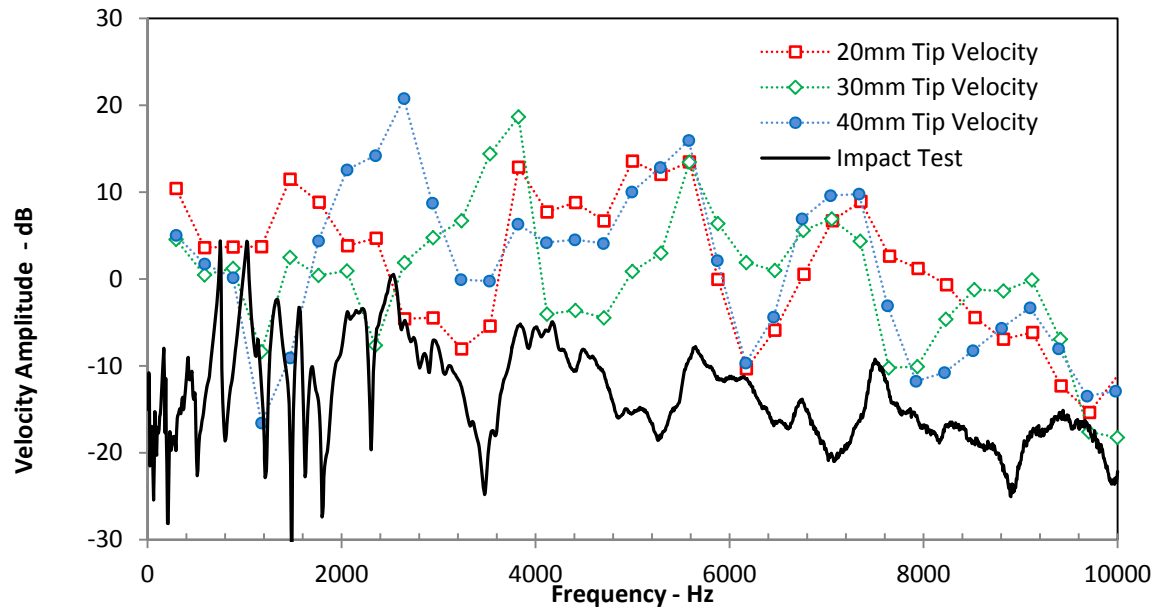


Figure 5b. Comparison of bow tip response for several values of bow to bridge distance to bow natural frequency determined by impact hammer test

These results show no evidence that the vibrational modes of the bow stick have any influence on the motion of the bowed string. Since the lower stick modes (below 2KHz) are lightly damped and have sharp peaks and troughs, it may just be a coincidence of these test conditions that no coupling is seen. It may be possible to observe such an effect under certain special conditions – for example when the harmonics of the bowed note exactly coincide with one or more of the bow’s resonant frequencies. This test has not been done yet. We know that bows sound different from each other. What is causing that difference if not their modal frequencies? This is perhaps the most important unresolved question about bows remaining to be answered.

### C. Transient Response

There is a startup transient at the beginning of the bow stroke, before the full establishment of Helmholtz motion which depends on bow speed, acceleration, distance from bridge and the bowing force [31]. As observed by Askenfeldt [20] the duration of this “pre-Helmholtz” transient increases as the bowing point approaches the bridge. As previously noted by other researchers [32, 24], the duration of this transient phase is not constant since it involves chaotic friction effects. To illustrate this variability, eight trials were made at the same test conditions [acceleration=1.5 m/sec,  $W=80g$  (785mN),  $B=30mm$  ( $\beta$  to center of hair ribbon  $\approx 1/13$ ),  $V=20$  cm/sec)]. These bowing parameters are approximately in the center of the Schelleng diagram [10] of acceptable bowing conditions. The average time to reach Helmholtz motion was 120 msec, with a standard deviation of 50 msec. The maximum and minimum values were 75 and 215 milliseconds respectively. Three representative data samples are shown in Figure 6. The upper curve achieves Helmholtz motion in the shortest time of the eight samples. After a period of multiple slipping (two events per period), steady Helmholtz motion is achieved after  $\sim 75$ msec.

The middle sample takes ~110 msec, which is close to the mean response time. The bottom sample does not reach steady motion until 215 msec, beyond the time range of the plot window.

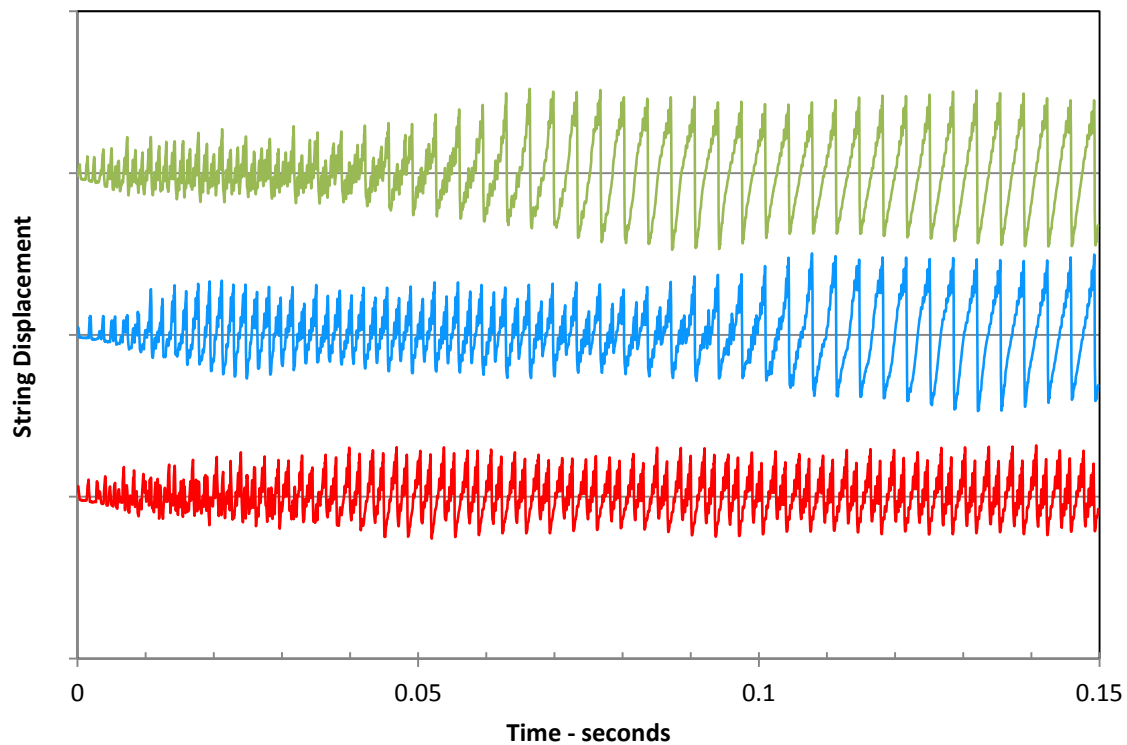


Figure 6. Samples illustrating the variation of the startup transient under the same test conditions: [acceleration=1.5 m/sec, V=20 cm/sec, W=80g (785mN), B=30mm ( $\beta$  to center of hair ribbon  $\approx 1/13$ )]

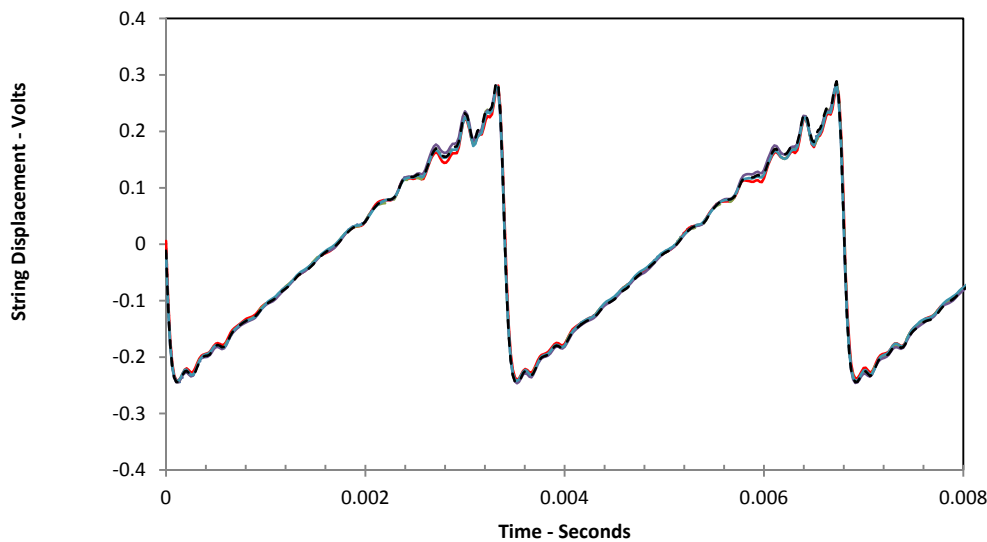
This inherent variability reinforces the need to measure the mean and standard deviation from multiple test samples, in order to properly quantify pre-Helmholtz transient behavior. While the acceleration is very repeatable, some of the variability of the string response may be due to nonlinear response of the machine, or the complex dynamic interaction between contact force and bouncing modes of the bow. Qualitatively, it was noted that during some downbows, the bow would bounce vertically at the start of the stroke. This causes a wider variability of pre-Helmholtz transient, since the contact force is dynamically altered during the bounce. Upbows, which bounce less and at a higher frequency, generally had less variability. These effects call for more study and are beyond the scope of this paper.

#### **D. Repeatability and Sources of Error**

In order to be useful for making comparisons, the output of any bowing machine must be repeatable and reproducible. Potential sources of errors include: misalignment of bow to bridge, uniformity of downward force and velocity over the length of the stroke, aging of hair and string, humidity, and rosin application on bow and buildup on string. A test of rosin buildup on string showed no change in the string response after 35 up/down bow strokes. Since the bow velocity

is measured at the motor, not directly at the bowing point, mechanical instabilities in the machine, such as friction or belt windup can cause errors in the velocity measurement. Inherent in any digital control system is also the potential for sampling and timing errors. Occasionally, the bow motion carriage would stick or jerk, but this condition is easily detected and those test runs were rejected and repeated.

To assess the validity of the machine and test procedure, the same bow was tested repeatedly over several days at identical conditions of speed, force and distance to bridge. Between tests, the bow was completely removed from the machine, re-mounted and all settings were re-adjusted. The relative humidity was 50-60% for these tests. Steady state results (after the startup transient) at the midpoint of the bow stroke for 6 down strokes are shown in Figure 7 (for 80g bow force, 20cm/sec velocity, 30mm from bridge). The time histories and FFT plots are virtually identical. The standard deviation,  $\sigma$  of the RMS levels is 1.1mV (0.07dBV) and for the spectral centroids, 24 Hz. Eight spectral averages were found to provide very repeatable results. These results provide confidence in the machine's reproducibility and repeatability for studying the steady state response of bowed string motion.



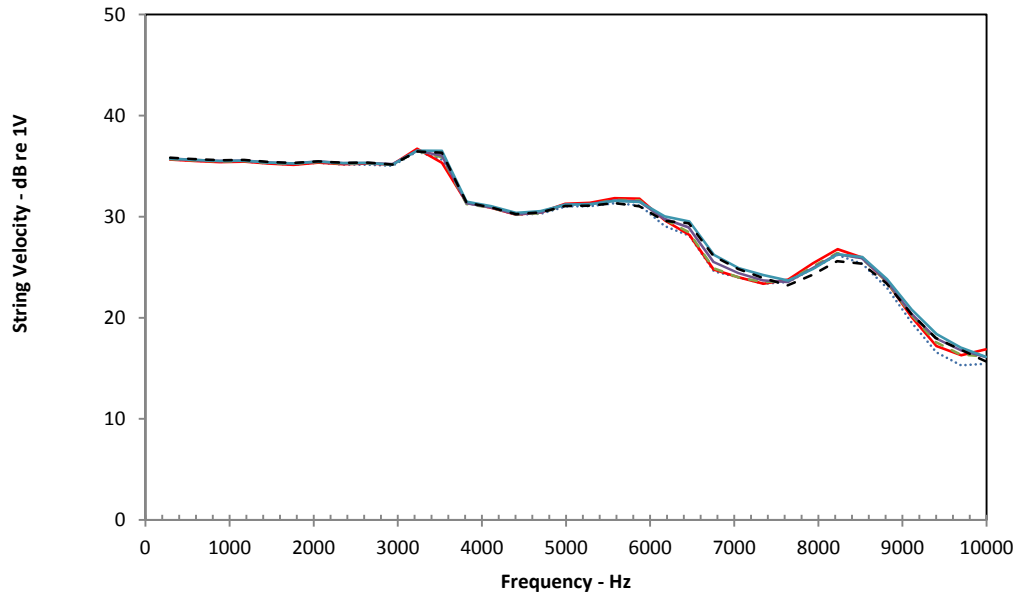


Figure 7. Repeatability of steady state bowed response for 6 repetitions of single bow strokes for the same bow and playing conditions, a) Time history ( $\sigma V_{rms}=0.07\text{dB}$ ), b) Peak frequency response ( $\sigma f_c=24\text{Hz}$ )

Unless otherwise noted, in all subsequent tests discussed in this paper, 1.20 seconds of data is analyzed (8 averages, each of duration 0.1498 seconds), centered around the middle of a down bow stroke, after the startup transients have died out.

### E. Effect of Bowing Parameters - Speed, Pressure, Bowing Distance

A trained violinist instinctively knows how to control bowing parameters (force, speed, bowing position) to achieve the desired tonal color. Several tests were conducted to quantify these effects, using the monocord with a Helicore D string. The same Pernambuco bow was used for all tests. Data was analyzed for a downbow stroke. To eliminate the effects of startup transients, all tests discussed below focus on a motion of 24cm centered about the midpoint of the bow.

#### Speed (V)

Bow speed was varied from 10-40 cm/sec for a constant downward force and distance from the bridge. As seen in Figure 8, bow speed has a large effect on the overall sound volume (as measured by the RMS voltage,  $V_{rms}$ ) and a moderate effect on the tone color (as measured by spectral centroid). Higher bow speed proportionally increases the volume and the low frequency relative to high frequency content (as measured by the spectral centroid). It is well known by violinists that increasing bow speed is the principal way to achieve greater volume of sound. These results are consistent with the published literature.



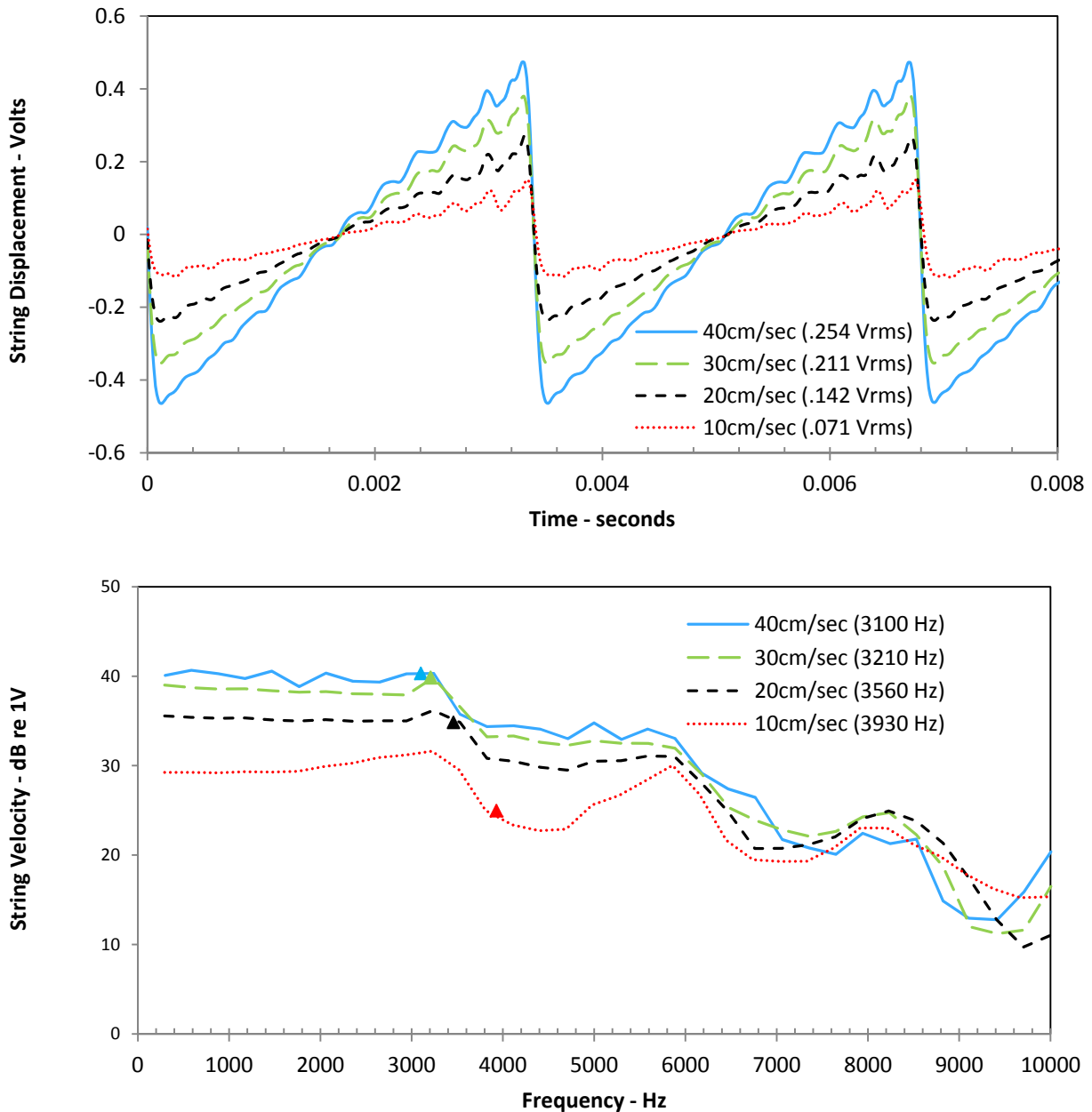


Figure 8. Effect of bowing speed,  $V$ , on steady state bowed response ( $W=80g$ ,  $B=30mm$  from bridge, measured 4.5mm from opposite bridge) a) Time history (RMS voltage in parentheses) b) Peak frequency response, FFT, (Frequency centroid location is in parentheses and indicated by triangles)

### Force ( $W$ )

Bowing force was varied from 40 to 100 grams while velocity and distance from bridge were held constant. As seen in Figure 9, increasing the force does not significantly change the amplitude of the wave or the overall volume, but it markedly increases the high frequency content. Higher values of force delay the onset of slip, causing sharper corners in the Helmholtz motion, thereby increasing the high frequency content and the spectral centroid. While the actual

volume may not change, the perceived loudness will increase because of the influence of the higher harmonics. These results are consistent with the published literature.

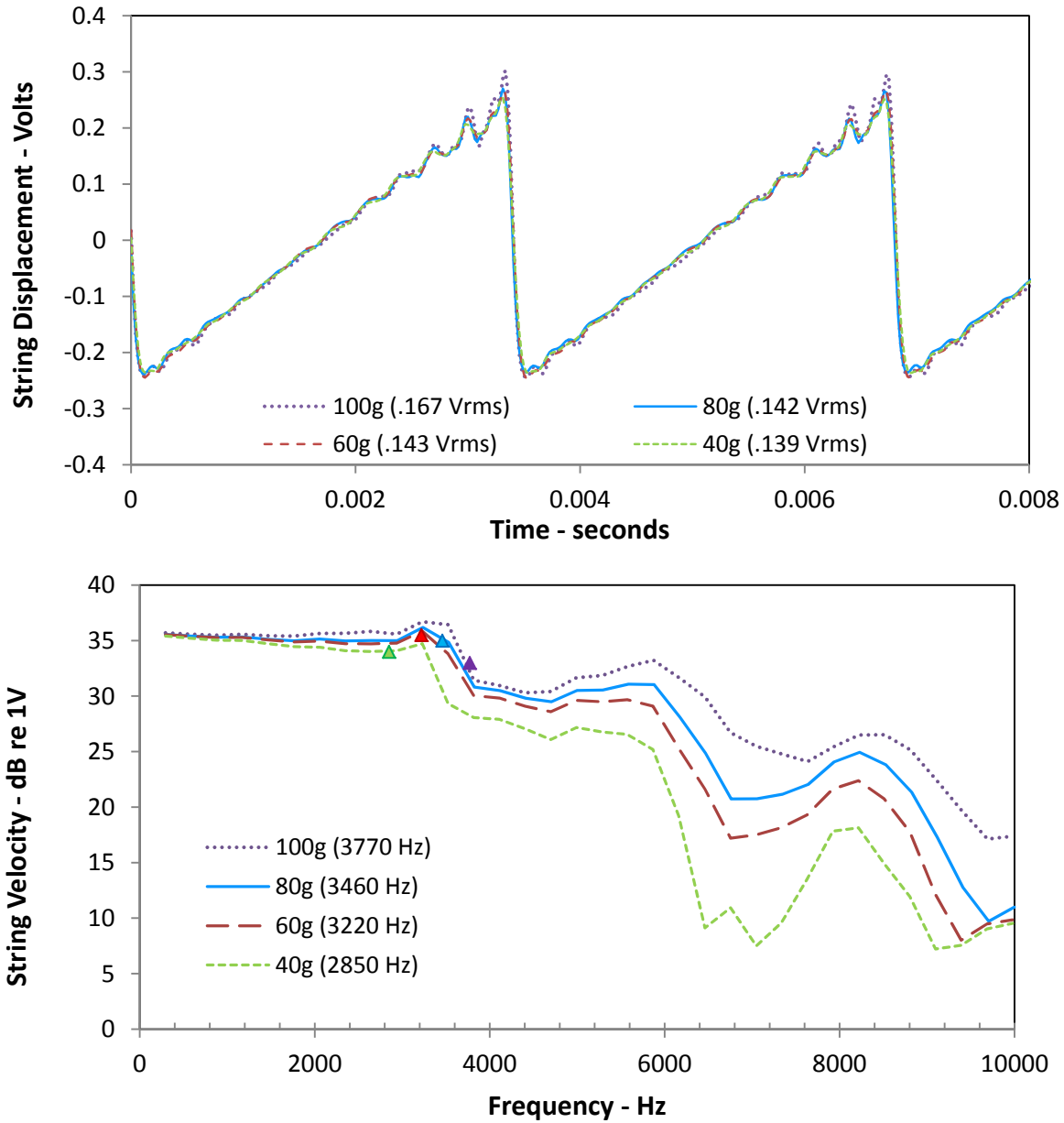
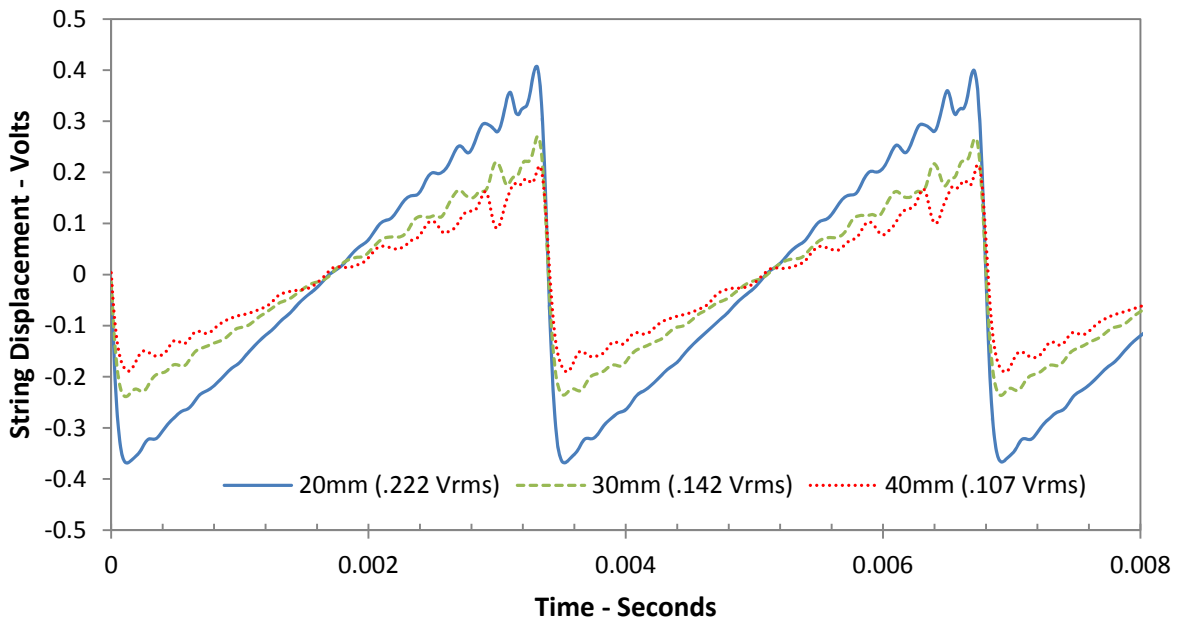


Figure 9. Effect of bowing force,  $W$ , on string displacement ( $V=20$  cm/sec,  $\beta=30$ mm) a) Time history (RMS voltage in parentheses) b) Frequency response, FFT, (Frequency centroid location is in parentheses and indicated by triangles)

## Bowing Position (B)

Bowing distance (B, measured from the far edge of the hair ribbon to the bridge) was varied from 20 to 40mm for a constant weight of 80g (0.78N force) and speed of 20cm/sec. As shown in Figure 10a, the overall amplitude of the string ( $V_{rms}$ ) increases proportionally when bowed closer to the bridge. The frequency response curves (Figure 10b) all exhibit the common feature of a relatively flat plateau at low frequency which extends to a “cut-off” frequency directly related to the bowing distance from the bridge, where the response rapidly rolls off. This width of this plateau increases as the string is bowed closer to the bridge. This agrees with the qualitative observation of players, that not only is it louder, but bowing closer to the bridge produces a more brilliant, focused sound. However, the spectral centroid suggests otherwise in this case - the frequency centroid actually decreases slightly as the bowing point moves closer to the bridge. A simple measure like spectral centroid may not be able to capture the perceptual differences between such complicated frequency spectra. These results do not agree with Guettler et al [33], who concluded that bow position does not change the spectral envelope.



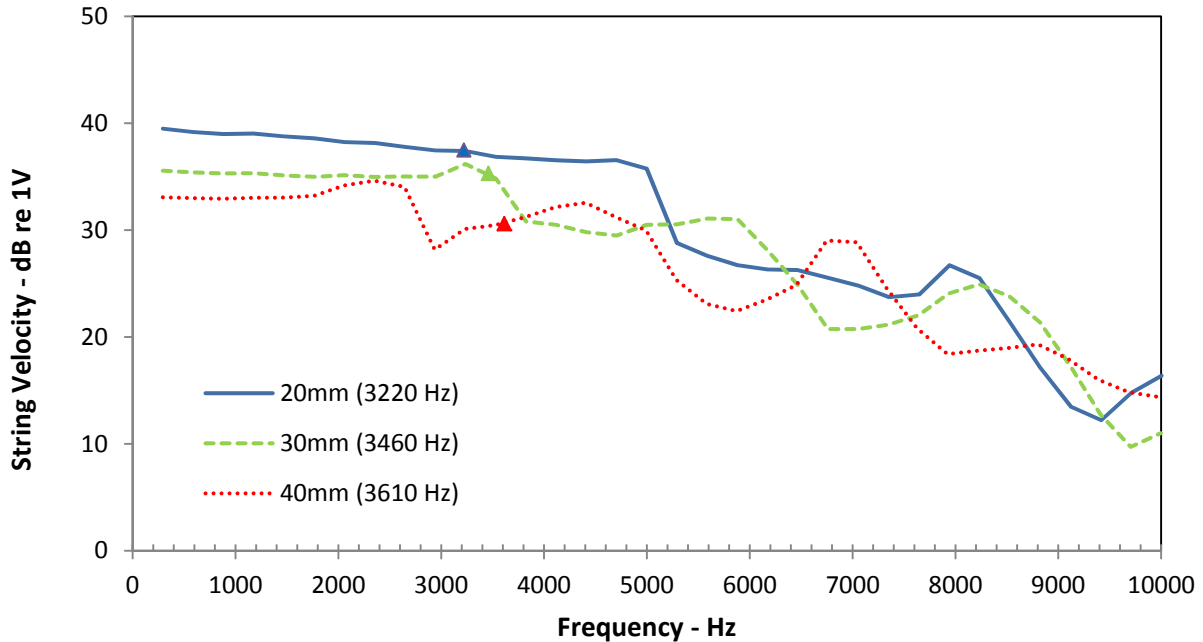


Figure 10. Effect of bowing distance from bridge, B, on steady state bowed response response [W=80g, V=20cm/sec], a) Time history (RMS voltage in parentheses) b) Frequency response, FFT, (Frequency centroid location is in parentheses and indicated by triangles)

## F. Discussion of Helmholtz motion

The theoretical “Helmholtz” string displacement is a sawtooth wave consisting of integer multiples of the fundamental frequency ( $1/T$ ). The amplitudes of the harmonics are proportional to  $1/n$ , where  $n$  is the index of the harmonic [36]. If the string is bowed at a nodal point of a string harmonic (when  $B/L = \beta$  is an integer value) and the width of the hair ribbon is small, periodic ripples are superimposed on the portion of the waveform where the bow hair is in contact with the string [37]. These are commonly called secondary or Schelleng ripples [10] and are the result of torsional and transverse disturbances reflecting between the bridge and the bowing point at a frequency at a frequency of  $1/\beta T$ . For the real case of finite width of hair, as first observed and called “crumples” by Helmholtz [7], any string harmonic which has a node that falls within the span of the hair will be attenuated. The frequency of these “crumples” increases as the bowing distance decreases. A good example of this effect can be seen in Figure 8a. For illustration, consider the case where the node falls exactly in the middle of the hair ribbon. During the sticking phase of the Helmholtz motion, half the hair will be trying to pull the string in the direction favoring the mode shape, while the other half will be pulling it in the direction opposing the mode. This is analogous to pushing equally downward on both sides of a playground see-saw – nothing happens. [38-40]

In the frequency domain, these regions of partial modal cancellation (“crumple zones”) are analogous to stop bands in the frequency response of a filter. Referring to the dashed curve in Figure 8b, for a bowing point 30mm from the bridge, the amplitude of the harmonics is relatively flat up to a “corner” at ~3200 Hz where it rolls off quickly. This corner occurs at the lowest frequency where a string node coincides with the far edge of the hair ribbon (when one half wavelength=30mm, at 3230 Hz). Up to this frequency, there is efficient spatial coupling between the standing wave pattern and the input from the bow hair. As frequency increases further, a node would occur within the hair ribbon, resulting in inefficient spatial coupling. A theoretical minimum will occur when a half wavelength of the string mode coincides with the middle of the hair ribbon, at 3880 Hz. As the node passes outside of the hair ribbon (above 4850 Hz) more efficient spatial coupling again occurs and the amplitude begins to rise. Another stop band would begin when the next node passes into the hair ribbon ( $\lambda=30\text{mm}$ , at 6460 Hz). As seen in Figure 10b, the critical frequency increases as the bowing distance decreases. The theoretical cutoff frequency for  $\beta=20\text{ mm}$  is 2422 Hz, and 4845 Hz for  $\beta=40\text{ mm}$ . These values agree well with the observed data in Figure 10.

The observed crumples actually represent subtraction from the theoretical Fourier Series components of a sawtooth wave. Figure 11 shows the result if just the 13<sup>th</sup> harmonic at 3820 Hz is completely deleted from a theoretical N wave - ripples of constant amplitude at the frequency of the deleted harmonic. This corresponds to the string harmonic that would have a node directly in the center of the hair ribbon. The measured waveform of string displacement shows a similar behavior from the middle to end of the sticking phase, but with ripples of increasing amplitude as time progresses. A possible physical explanation is that during the sticking phase, each cycle of the affected mode will be successively diminished by localized friction as the string rotates relative to the bow hair [41]. As the harmonic is progressively attenuated from the measured sawtooth wave, the ripple amplitude would appear to grow. The frequency of the small ripples at the beginning of the sticking phase are consistent with a secondary wave.

The result of these regions of partial cancellation are dips and humps in the frequency response above the cutoff frequency, with locations determined by the bowing distance. Other authors [16,36] have observed the first transition in frequency content (called the “cutoff” frequency here), but the existence of multiple regions of partial cancellation has not been reported or explained before.

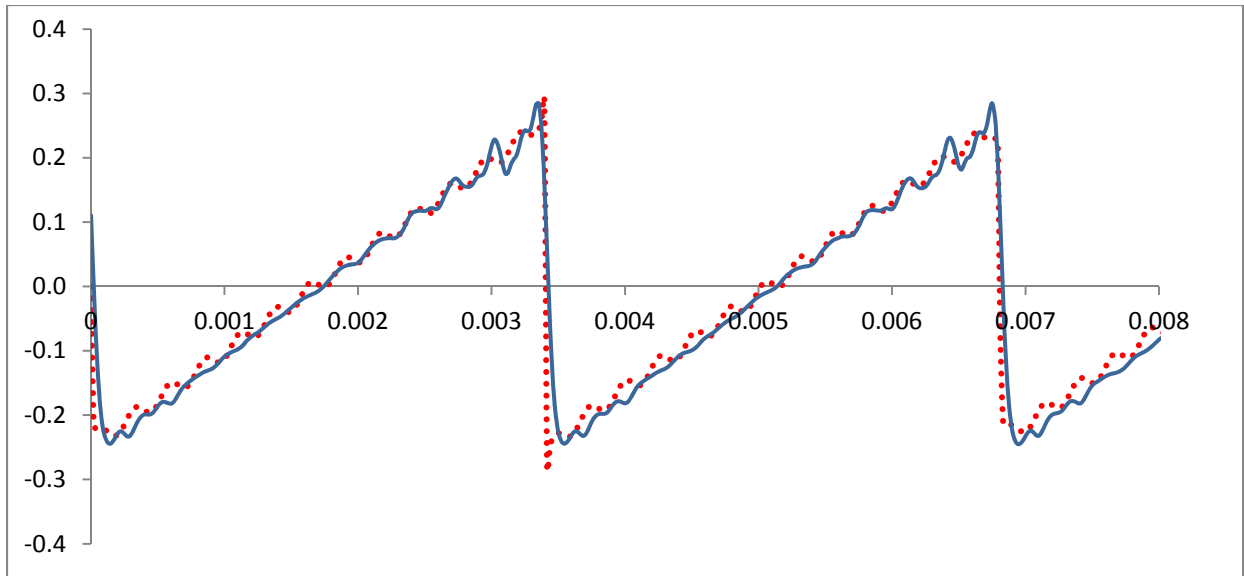


Figure 11. Solid blue curve is measured time history of string motion, dotted red curve is Fourier series reconstruction of N wave with the 13<sup>th</sup> harmonic deleted, (B=30mm)

### G. Comparison of Different Bows

This machine allows comparison of different bows under the exact same playing conditions, which is impossible to achieve with a human player. In an attempt to find measurable dynamic quantities that can be related to playability – an acoustic signature, eight bows were studied. They were carefully chosen to represent a wide variety of quality, value and construction materials (Pernambuco, Brazilwood, graphite, steel). One bow is from the golden age of French bowmaking (Dominique Peccatte), three are from fine modern makers (Noel Burke, Rodney Mohr, Morgan Andersen); two are modern graphite bows (Coda Prodigy and Rolland Spiccato); and another is made of hollow steel (Heddon, a fishing rod manufacturer from the 1940's). The A. Schmidt bow is the cheapest available factory-made Brazilwood bow from China (\$60).

Table I. Mechanical properties of test bows

Bow	Material	Weight (g)	Lucchi (m/s)	CG (cm)	Moment of Inertia w.r.t frog (g-cm <sup>2</sup> )	Center Deflection to 1# load (inch)
Morgan Andersen	Pernambuco	60.9	5320	25.6	51100	.177
Noel Burke	Pernambuco	60.9	5360	26.9	55150	.168
Coda Prodigy	Carbon fiber	61.0	5490	26.2	56900	.132
Heddon	Steel, hollow	55.8	4740	27.5	59700	.147
Rodney Mohr	Pernambuco	60.8	5390	25.6	52050	.174
Dominique Peccatte	Pernambuco					
Rolland Spiccato	Carbon fiber	63.8	5210	25.6	59100	.175
A. Schmidt	Brazilwood	65.9	4840	27.0	61200	.225

The results for 80g force, 20cm/sec velocity and bowed 30mm from the bridge are shown in Figure 12. Numerical values for  $V_{rms}$  and spectral centroid are listed in Table 1. The string displacement shown in Figure 11 is virtually identical for each bow. The frequency response of the string velocity reveals small differences in the higher frequency range and in the frequency centroid. Preliminary results from an ongoing subjective listening test indicate that these differences are audible.

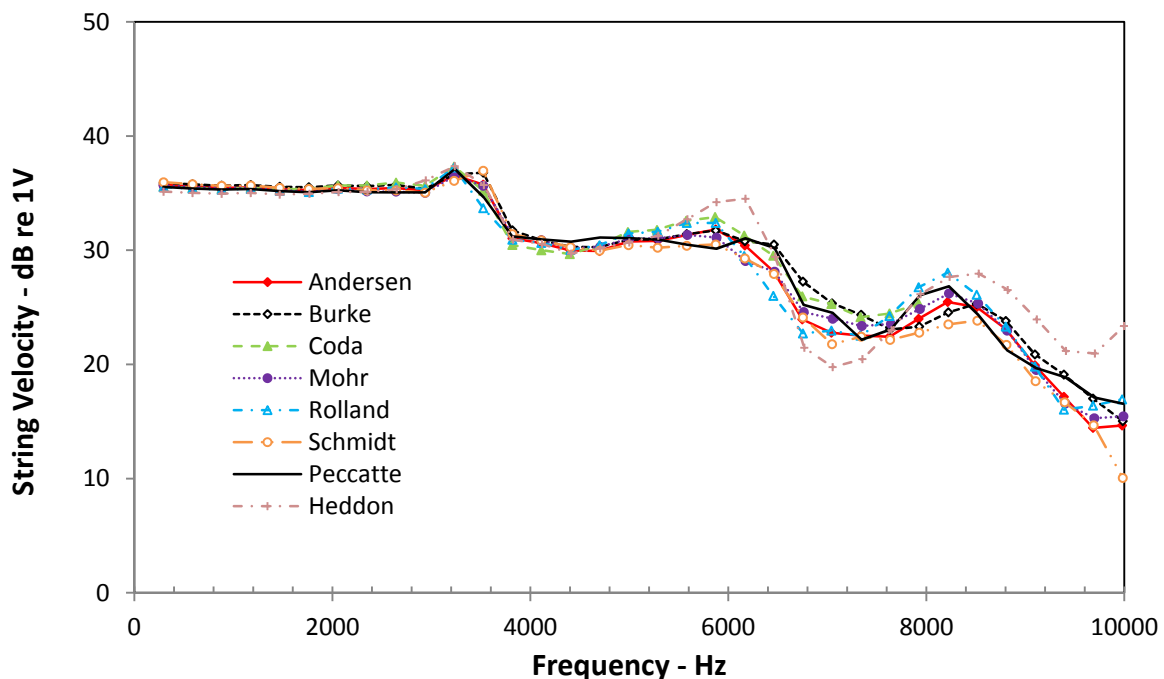
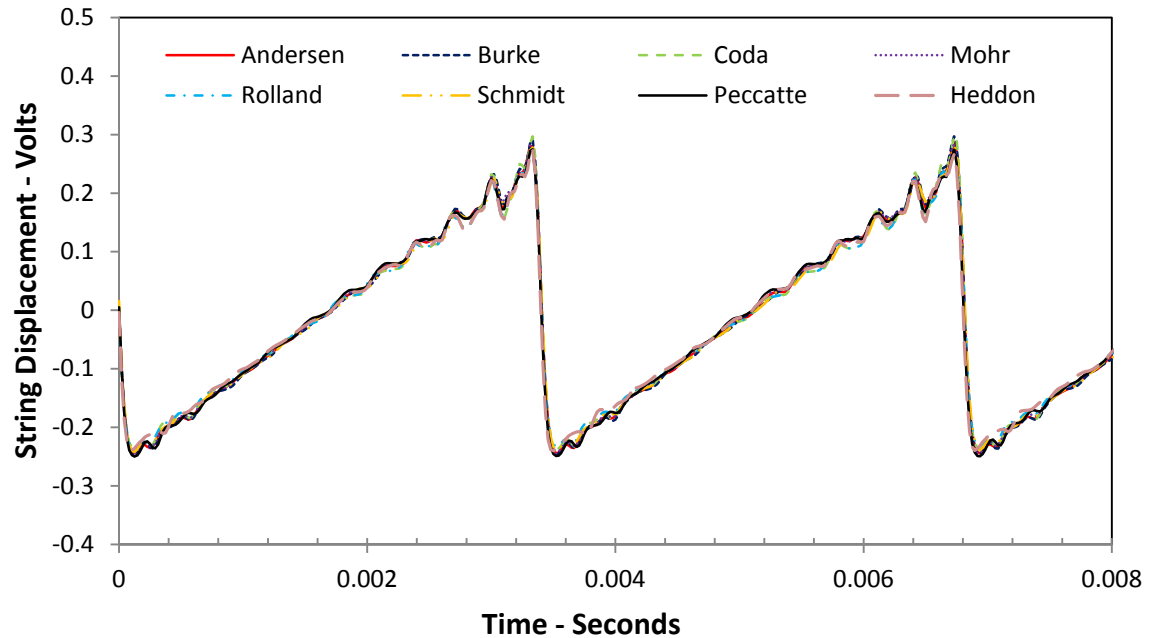


Figure 12. Steady state bowed response for different bows under the same playing conditions [W=80g, V=20 cm/sec, B=30mm] a) Time history b) Frequency response

As seen in Table II, the overall amplitude (dBVrms) of the string response is virtually the same for each bow (standard deviation = 0.26dB). The frequency centroid for the string velocity varies across the bows by ~300 Hz (standard deviation 108Hz). These variations are well beyond the observed repeatability for a single bow (see Figure 5). The hollow steel bow has the lowest overall volume and the highest frequency centroid. The graphite bows also have relatively higher frequency centroids than those made of Pernambuco. Wider variations from bow to bow are seen in the tip for overall volume and frequency centroid. There is very low correlation between the overall volume and the frequency centroid of the string velocity. Further, there is no significant correlation between the vibrations of the tip and the string. This lends further support to the conjecture of previous researchers [21] that the internal dynamics of the bow have minimal, if any effect on the bowed motion of the string when speed, pressure and position are precisely controlled. However, the dynamic and static properties of the bow are obviously extremely important to players, providing tactile feedback which allows precise control of bowing parameters to achieve the desired playing effect.

Table II. Comparison of different bows for the same playing conditions (W=80g, V=20cm/sec, B=30mm)

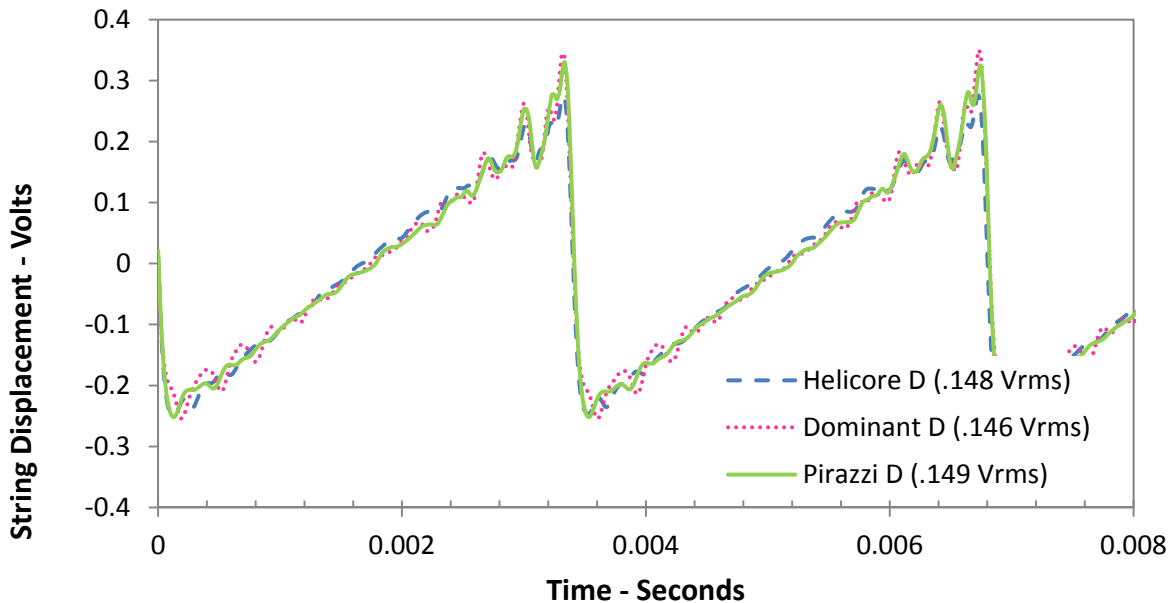
Bow	Material	String Response		Bow Tip Response	
		Displacement (dB Vrms)	Frequency Centroid of Velocity (Hz)	Acceleration (dB Vrms)	Frequency Centroid of Velocity (Hz)
Morgan Andersen	Pernambuco	-16.74	3585	-17.17	4587
Noel Burke	Pernambuco	-16.57	3651	-16.39	4120
Coda Prodigy	Carbon fiber	-16.81	3773	-17.20	4093
Heddon	Steel, hollow	-17.34	3789	N/A sensor failure	N/A sensor failure
Rodney Mohr	Pernambuco	-16.78	3621	-18.41	4488
Dominique Peccatte	Pernambuco	-16.90	3670	-20.13	4556
Rolland Spiccato	Carbon fiber	-16.96	3673	-20.11	3978
A. Schmidt	Brazilwood	-16.57	3476	-18.85	4550
	<b>Mean</b>	<b>-16.8 dB</b>	<b>3653 Hz</b>	<b>-18.0 dB</b>	<b>4303 Hz</b>
	<b>Standard Deviation, <math>\sigma</math></b>	<b>0.26 dB</b>	<b>108 Hz</b>	<b>1.36 dB</b>	<b>268 Hz</b>

## H. Comparison of Different String Brands

Three medium tension D strings from different manufacturers (D'Addario Helicore, Tomastik Dominant and Pirastro Eva Pirazzi) were tested with the bowing machine at identical playing conditions. As illustrated in Figure 12, there is little difference in the overall volume (as seen in



the wave amplitude and measured by Vrms), but significant difference in the frequency content (as seen in the frequency response plot and spectral centroid value). The specifications of these strings, derived from manufacturer's data are listed in Table III. These strings differ greatly in their construction. Helicore has a stranded steel core, surrounded by a copper wire interwoven with a polymer, with a flat aluminum outer-wrap. By design, it is intended to have a viscous damping characteristic and its smaller diameter will diminish torsional vibrations. The Dominant and Eva Pirazzi strings consist of a stranded polymer core covered by three flat aluminum windings. This type of construction provides non-linear friction damping, caused by relative motion between the winding layers. Unfortunately, manufacturers do not publish data on bending stiffness or damping, properties which would have a great effect on their frequency response. By qualitative observation, the Helicore strings have the lowest bending stiffness and the most even response with frequency. The Pirazzi and Dominant strings appear to have less damping in the 5-6KHz region. Any other conclusions are difficult to make. However, as compared to the effect of changing bows, changing the string brand can cause a far larger difference in the string motion, and presumably the radiated sound.



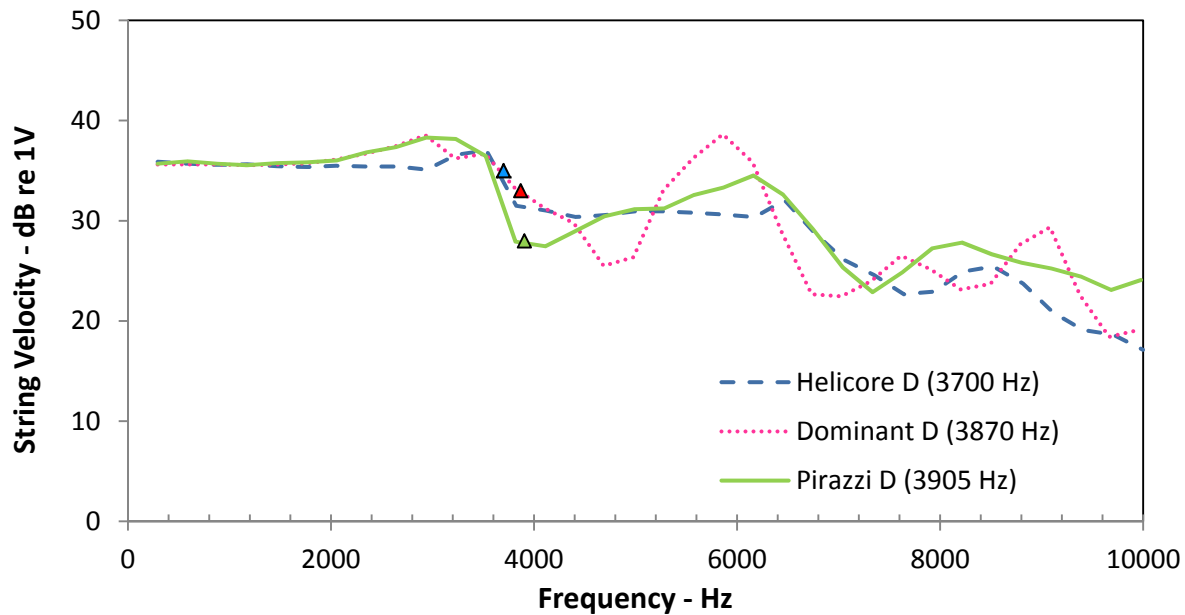


Figure 13. Steady state bowed response for three different string brands [W=80g, V=20cm/sec, B=30mm] a) Time history (RMS voltage in parentheses) b) Frequency response, FFT, (Frequency centroid location is in parentheses and indicated by triangles)

**Table III.** Physical properties of medium tension violin D strings, from manufacturer’s tension data and physical measurement (f=294 Hz, L=328 mm)

String Brand	Tension, T (N)	Lineal Density $\rho=T/(2Lf)^2$ (mg/cm)	Impedance $Z=\sqrt{T\rho}$ (kg/s)	Dia (mm)	Core material
Tomastik Dominant	40.5	10.90	0.210	0.80	Stranded Polymer
Pirastro Eva Pirazzi	47.4	12.75	0.246	0.67	Stranded Polymer
D’Addario Helicore	51.2	13.77	0.266	0.60	Stranded Steel

#### IV. CONCLUSIONS

The bowing machine described in this paper provides precisely controlled, reproducible bowing motion. It makes possible detailed studies of string and bow response. It is also a very useful tool for producing audio files to be used in subjective listening tests. Results using this machine show that, for steady Helmholtz string motion measured on a monocord (disregarding the startup transient):

1. There is no significant correlation between bow tip vibration and string motion.

1. Increasing bow force has little effect on overall amplitude of the string vibration, but sharpens the corner of the Helmholtz wave, increases the high frequency content, and raises the spectral centroid.
2. Higher bow speed increases the amplitude of the string vibration, while lowering the spectral centroid.
3. Bowing closer to the bridge increases the string amplitude, alters the spectral content, and causes a small decrease in the spectral centroid.
4. When played under identical conditions, bows of drastically different physical properties and monetary value result in small differences in steady-state string motion, and larger differences in bow tip vibration. Preliminary results from an ongoing subjective listening test indicate that these differences are audible.
5. Changing the string brand can have a larger effect on the string vibration than using a different bow.

Future studies will use this machine to examine in greater depth: the startup transient; the interaction between bow natural frequencies and string motion; the interaction of bow and violin dynamic properties; and the effects of humidity, rosin, hair tension, and hair aging.

### Acknowledgements

The author wishes to thank Norman Pickering for providing inspiration, encouragement and advice.

### References

1. C. Gough, "The violin bow: Taper, camber and flexibility", *J Acoust Soc Am* **130**, 4105-4116, (2011).
2. C. Gough, "Violin bow vibrations", *J Acoust Soc Am* **131** 4152-4163, (2012).
3. J.E. Graebner and N. Pickering, "Taper and camber of violin bows", *J Violin Soc Am*, **22**(1), 160-168, (2009).
4. G. Bissinger, "Bounce tests, modal analysis and playing qualities of violin bow", *Catgut Acous. Soc. Jnl (Series II)* **2**, 17-22 (1995).
5. F. Ablitzer, J.P. Dalmont and N. Dauchez, "Static model of a violin bow: influence of camber and hair tension on mechanical behavior", *J Acoust Soc Am* **131**(1) Pt.2, 773-782 (2012).
6. A. Askenfelt, "Observations on the dynamic properties of violin bows", *STL-QPSR* vol 33(4), 43-49, (1992). This is available online at <http://www.speech.kth.se/qpsr> (date last viewed 29 May 2014).
7. H. Helmholtz, *On the Sensation of Tone*, 1885 English translation, (Dover Publications, NY, 1954).

8. C. V. Raman, "Experiments with mechanically played violins", in Proc. Indian Assoc. for the cultivation of Sci. 6, 1920, reprinted in *Benchmark Papers in Acoustics*, Vol 5., Part I, edited by C. M. Hutchins, 19-36, (Dowden Hutchinson and Ross, Stroudsburg PA,1975).
9. F. A. Saunders, "The mechanical action of violins", *J.Acous.Soc.Am.*, **9**(20), 81-98 (1937).
10. J. C. Schelleng, "The bowed string and the player", *J.Acous.Soc.Am.*, **53**(1), 26-41 (1973).
11. Meinel, Hermann, " über Frequenzkurven von Geigen", *Akust. Z. 2*, p 22-33 (1937).  
Reprinted in *Benchmark Papers in Acoustics* vol. 5 Musical Acoustics, Part 2, pp 161- 172. Dowden Hutchinson and Ross Inc. 1973.
12. J. Bradley and W. Stewart, "Comparison of violin response curves produced by hand bowing, machine bowing and an electromagnetic driver", *J.Acous.Soc.Am* **48**(2) Part 2, 575-578, (1970).
13. L. Wang and C. Burroughs, "Acoustic radiation from bowed violins", *J.Acous.Soc.Am* **110**(1), 543-555, (2001).
14. B. Bladier, "Contribution a l'etude des cordes du violoncello," *Acustica* **11**(6), 373-384, (1961).
15. B. Lawergren, "On the motion of bowed violin strings", *Acustica*, **44**, 195-206, (1980).
16. N. Pickering, *The Bowed String*, 132 pages,(Amereon Ltd. Publisher, Mattituck, NY, 1991).
17. R. T. Schumacher, "Measurements of some parameters of bowing", *J.Acous.Soc.Am*, **96**(4), 1985-1998, (1994).
18. A. Cronhjort, "A computer-controlled bowing machine (MUMS)", Summary of M.S. thesis at Swedish Royal Institute of Technology, KTH Royal Institute of Technology,, STL-QPSR vol. 2-3, pp. 61-66, (1992). This is available online at <http://www.speech.kth.se/qpsr> (date last viewed 29 May 2014) .
19. E. Schoonderwaldt , K. Guettler and A. Askenfelt, "An empirical investigation of bow-force limits in the Schelleng diagram", *Acta Acust United Ac* **94**, 604-22, (2008).
20. K. Guettler and A. Askenfelt, "Acceptance limits for the duration of pre-Helmholtz transients in bowed string attacks", *J Acous Soc Am*, **101**(5), 2903-2913, (1997).
21. K. Guettler and A. Askenfelt, "Some aspects of bow resonances- conditions for spectral influence on the bowed string", KTH Royal Institute of Technology, STL-QPSR vol 36, 107-118, (1995). This is available online at <http://www.speech.kth.se/qpsr> (date last viewed 29 May 2014).
22. R. Schumacher , S. Garoff and J. Woodhouse, "Probing the physics of slipstick friction using a bowed string", *J Adhesion* **81**, 723-750, (2005).
23. J. Woodhouse, R. Schumacher and S. Garoff , " Reconstruction of bowing point friction force in a bowed string", *J Acoust Soc Am* **108**, 357-368, (2000).
24. P. Galluzzo, "On the playability of stringed instruments", Ph.D. Thesis University of Cambridge (2003).
25. P. Galluzzo and J. Woodhouse, "High performance bowing machine tests of bowed string transients", *Acta Acust United Ac* **100**, 139-153, (2014).

26. A. Askenfelt, "Measurement of the bow motion and bow force in violin playing", *J Acoust Soc Am* **80**, 1007-1015, (1986).
27. A. Askenfelt, "Measurement of the bowing parameters in violin playing: II Bow bridge distance, dynamic-range and limits of bow force", *J Acoust Soc Am* **86**, 506-513, (1989).
28. E. Schoonderwaldt and M. Demoucron, "Extraction of bowing parameters from violin performance combining motion capture and sensors", *J Acoust Soc Am* **126**, 2695-2708, (2009).
29. W. Reinicke, Dissertation, Institute for Technical Acoustics, Technical University of Berlin, 1973
30. N. Harris and F. Fahy, "A comparative study of the hammered bridge response and the bowed violin response of the violin", *J Violin Soc Am*, **22**(1), 210-223, (2009).
31. G. Peeters, "A large set of audio features for sound description", Institut de Recherche et Coordination Acoustique/Musique (IRCAM) technical report in English, pp 1-25, (2003). This is available online at <http://www.ircam.fr> (date last viewed 29 May 2014).
32. E. Schoonderwaldt, "The Violinist's Sound Palette: Spectral Centroid, Pitch Flattening and Anomalous Low Frequencies", *Acta Acust United Ac* **95**, 901-914, (2009).
33. J. Woodhouse and P. Galluzzo, "The bowed string as we know it today", *Acta Acust United Ac* **90**, 579-589, (2004).
34. R. T. Schumacher and J. Woodhouse. "The transient behaviour of models of bowed-string motion", *Chaos* **5**, 509-523 (1995).
35. K. Guettler, E. Schoonderwaldt and A. Askenfelt, "Bow speed or bowing position – which one influences the spectrum the most?" Proceedings of Stockholm Music Acoustics Conference (SMAC 03), Stockholm, Sweden, 4 pp. (2003).
36. A. Benade, *Fundamentals of Musical Acoustics*, Second Edition, pp. 505-525 (Dover Publications, NY, NY, 1990).
37. L. Cremer, *The Physics of the Violin*, pp. 5-198 (MIT Press, Cambridge, MA, 1983).
38. M. McIntyre, R. Schumacher and J. Woodhouse, "Aperiodicity in bowed-string motion", *Acustica* **49**, 13-32, (1981).
39. R. Pitteroff and J. Woodhouse, "Mechanics of the contact area between a violin bow and a string. Part II: Simulating the bowed string", *Acustica* **84**, 744-757, (1998).
40. R. Pitteroff and J. Woodhouse, "Mechanics of the contact area between a violin bow and a string. Part III: Parameter dependence", *Acustica* **84**, 929-946, (1999).
41. M. McIntyre and J. Woodhouse, "Fundamentals of Bowed-String Dynamics", *Acustica* **43**, 93-108, (1979).